

# Simulation-Based Design of Hybrid Particle Dampers with Application to Flexible Multibody Systems



Niklas Meyer and Robert Seifried

## 1 Introduction

Passive damping techniques are often used to reduce structural vibrations. Classical liquid dampers are mostly seen for these applications. These dampers are well studied and mathematically easy to describe. However, liquid dampers perform insufficiently under extreme temperatures, due to the change of viscous properties, and do need an anchor point. Hence, for applications where liquid dampers are not suitable, particle dampers are becoming more and more popular.

*Particle damping* (PD) technology is classified as an auxiliary-mass type vibration technique [1]. Either containers attached to the vibrating structure or holes within the vibrating structure are filled with a granular material of convex or non-convex shape. Various different materials like steel, tungsten, carbide, polymers and many more can be used. The particle size normally ranges from the micrometer scale to the millimeter scale. Thus, from several dozens up to millions of particles might be included in a single particle damper. By structural vibrations, momentum is transferred to the granular material causing granular movement. By particle interactions, energy dissipation occurs due to inelastic normal collisions and frictional losses. This reduces the structural vibrations.

Compared to other damping techniques, particle dampers show various advantages due to their conceptual simplicity and passive nature. They are cost-efficient devices, do not need an anchor point, and do not often degrade in time [2]. Using appropriate particles, e. g. steel or tungsten, particle dampers can even operate in extreme environmental conditions [1, 3, 4]. Furthermore, particle dampers add only

---

N. Meyer (✉) · R. Seifried  
Institute of Mechanics and Ocean Engineering, Hamburg University of Technology, Eißendorfer  
Straße 42, 21073 Hamburg, Germany  
e-mail: [n.meyer@tuhh.de](mailto:n.meyer@tuhh.de)

R. Seifried  
e-mail: [robert.seifried@tuhh.de](mailto:robert.seifried@tuhh.de)

little mass to the primary system [2] causing no significant change in its mass and stiffness [5]. It is also reported that particle dampers can be applied to a wide frequency range [6].

Although particle dampers show huge potential, they are so far only rarely used in technical applications. The major reason for this is that currently there exists no easy design guideline, which is due to their nonlinear behavior and the variety of influence parameters. These influence parameters strongly affect the particle motion, also called state of matter or *motion mode* (of the rheology behavior), which correlates in a non-trivial way with the damper's energy dissipation. These correlations are often only poorly understood, leading to a trial and error-based design process of particle dampers even nowadays. In [7], a systematic multiscale design methodology in form of a *toolchain* is developed, which is based on computational models as well as models derived from experiments. These models are extremely useful for supporting the damper design and damper integration on a structure. In addition, they also provide useful insights into the complex processes, the nonlinear effects, and the design parameters influencing the efficiency of particle dampers.

Within this paper, the toolchain is used to develop single particle damper units with predefined characteristics, which do not rely on a specific application. Different hybrid damper approaches are utilized to increase the efficiency of the individual particle dampers. Multiple container layers with different filling ratios are used to obtain an optimized damping behavior for transient vibrations. Inner structures within the dampers show a more robust behavior and buffering the damper's walls with a polymer leads not only to a considerable noise reduction, but leads also to an increased efficient range of operation.

This paper summarizes the research on the DFG projects SE1685/5-1 and 424825162 within the SPP1897. This paper is based on the publications [7–16] which originated from the two project phases and is organized in the following way: In Sect. 2 the systematic multiscale design methodology in form of a toolchain is presented. In the following sections the design toolchain is applied to design particle dampers for horizontal free and forced vibration systems of low intensity, see Sect. 3 and horizontal and vertical forced vibration systems of high intensity, see Sect. 4. Finally, the conclusion is given in Sect. 5.

## 2 Design Toolchain

Particle dampers show a nonlinear dynamical behavior, starting at the micro-mechanical effects during single particle impacts and sliding contacts, continuing with the energy dissipation inside the particle container, and ending at the interaction within a structure. For a better understanding, and thus also for the design of particle dampers, investigations on these different scales or levels, respectively, are necessary. A systematic multiscale design methodology in form of a toolchain is therefore developed, see Fig. 1 and [7]. Insights made on one level can be used on the next level to better understand the dynamical properties and shorten the

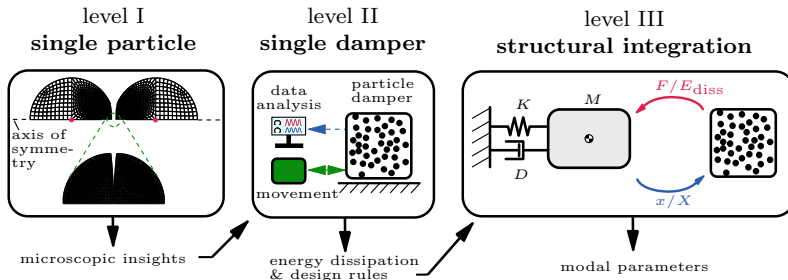


**Fig. 1** Toolchain for the analysis of particle dampers

overall design process of particle dampers. On all levels, numerical models, as well as experimental tests, might be used for analysis.

On the **first level** of the toolchain, the micro-mechanical behavior of single particle–particle and particle–wall interactions is analyzed. This provides important input for the second level. The **second level** represents investigations into an isolated particle damper subjected to a harmonic motion and the determination of the damper’s energy dissipation for a given excitation frequency range and amplitude range. First design rules and, if applicable, analytical formulas for the energy dissipation are derived here. Finally, the **third level** represents the integration of the particle damper in a vibrating structure to evaluate the overall damping effect.

## 2.1 Level I

The **first level** of the toolchain, see Fig. 1-single particle, is completely independent of the other two levels. On this level, the micro-mechanical behavior during a normal impact of two bodies of macroscopic size, like particle–particle or particle–wall, is analyzed. Here, a particle collides in a defined manner with the collision partner. Thereby, the energy dissipation during the impacts is of major interest and can mainly be characterized by the *coefficient of restitution* (COR)  $\varepsilon$  describing the velocity change during contact [17, 18]. The COR designates the quotient between the velocities right after (1) and before (0) the impact for the bodies I and II as  $\varepsilon = - (v_I^1 - v_{II}^1) / (v_I^0 - v_{II}^0)$ . For  $\varepsilon = 1$  the impact is called elastic. For  $\varepsilon = 0$  it is called fully inelastic and both collision partners move with the same velocity afterward.

In *discrete element method* (DEM) simulations, which are used on **level II**, often a constant COR is applied. However, the impact velocity of the collision partners has a big influence on the COR and should thus be considered. Numerical and experimental models can be used to determine the COR [19–21]. For example, Fig. 2 shows the experimental setup for the impact of a steel sphere against different planar wall materials, as detailed discussed in [14, 16]. The testbed consists of a steel sphere

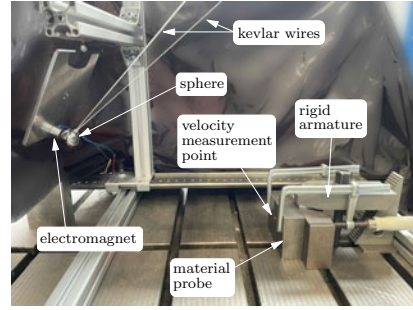
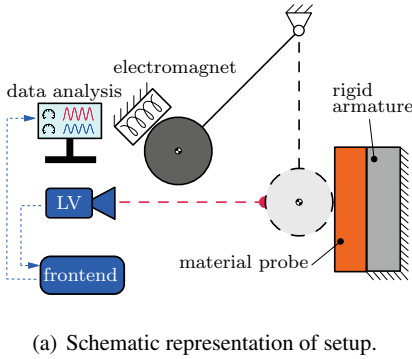


**Fig. 2** Test bed to determine the COR for a sphere–wall contact

of 15 mm radius which is suspended by thin wires impacting the wall material probe glued or fixed to a rigid steel block.

The sphere is held in the deflected state by an electromagnet. As the position of the electromagnet is variable, different impact velocities are achieved. After release, the velocity of the sphere is measured by the laser vibrometer (LV) PSV-500 from POLYTEC with a sampling frequency of 250 kHz.

Alternatively, numerical investigations using the *finite element method* (FEM) can be performed for determining the COR [20, 22]. A schematic representation of the sphere–sphere FEM model is shown in Fig. 1–level I. Here, for example, the spheres have an initial radius of 5 mm, which can be scaled to different sizes. Each sphere consists of 6093 axis symmetric 2D elements, called CAX4R in ABAQUS. The element size varies between 0.015 mm to 0.5 mm and both spheres are assigned with half the impact velocity with opposed signs [14, 16].

The analyzed steel–steel and steel–aluminum contacts show a high dependency on impact velocity [14, 16]. Exemplary, in Fig. 3a the experimental and numerical COR results for steel sphere–steel wall impacts are shown. These start at high COR values for low impact velocities and show a digressive decay towards higher impact velocities. Due to plastic deformations, repeated impacts onto the same spot show a much higher COR [22]. The FEM simulations are capable to reproduce the quantitative progression of the COR observed in experiments. Only small quantitative differences remain.

Besides the metal–metal impacts, steel–polymers combinations are investigated. Exemplary, in Fig. 3b the experimental and numerical COR results for steel sphere–polymer wall impacts are shown. The steel–polymer contacts show only little dependency on impact velocity. For  $v_1^0 > 0.1 \frac{m}{s}$ , only a little linear decrease of COR with impact velocity is observed. The effect of repeated impacts vanishes [16], as no plastic deformations in the contact zone occur. Numerically, a good agreement with the experimental measurements is achieved for low impact velocities, i. e.  $v_1^0 < 1 \frac{m}{s}$ . At high impact velocities, bigger differences are seen.

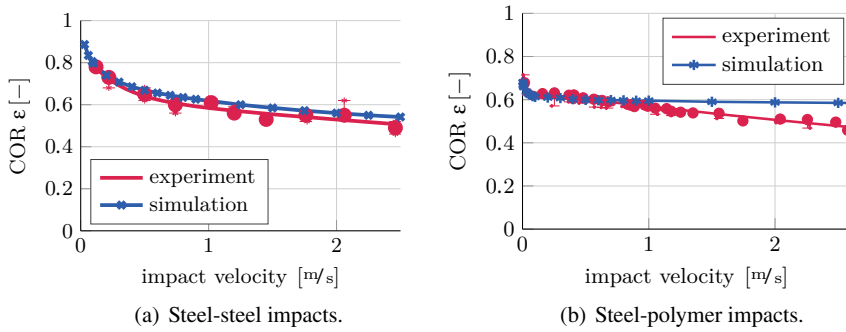


**Fig. 3** Experimental and numerical COR results for sphere-wall impacts of different materials

Using the validated numerical models, the CORs for various sphere diameters are calculated, which can be used for later DEM simulations. Indeed, it turns out that the dependency on impact velocity is much bigger than on the sphere's diameter. See [16] for further details.

## 2.2 Level II

The **second level** of the toolchain, see Fig. 1-single damper, represents investigations of an isolated particle damper subjected to a defined horizontal or vertical vibration. The energy dissipation of the particle damper is determined for the given excitation frequency range and excitation amplitude range. Additional, insights about the movement of the particle bed, called *motion mode*, are gained. The particle container is excited by a harmonic motion using a rheonomic constraint  $x_c = X \sin(\Omega t)$ , with container amplitude  $X$  and angular frequency  $\Omega = 2\pi f$ . The corresponding container velocity and acceleration follow as  $\dot{x}_c = V \cos(\Omega t)$  and  $\ddot{x}_c = -A \sin(\Omega t)$  with  $V = X \Omega$  and  $A = X \Omega^2$ . The dimensionless excitation intensity is defined as  $\Gamma = A/g$  with  $g$  as gravity constant. From the velocity of the particle container and the excitation force, the *complex power* can be determined. Using the complex power, the energy dissipation and the reduced loss factor are obtained, displayed as characteristic diagrams over the excitation frequency and excitation amplitude. These characteristic diagrams are also called *effective fields* in the following. The calculated effective fields can be stored and used on the third level of the toolchain for the integration process of the particle dampers in a vibrating structure. If applicable, the effective fields might be approximated by an analytical formula, which can also be integrated on the next level. All these aspects help to shorten the design phase on **level III**.

Investigations can be performed experimentally using a closed-loop controlled shaker setup or a linear drive. This depends on the excitation frequency and amplitude,

see e. g. [12, 14, 15]. Investigations can also be performed numerically using the DEM, see e. g. [7]. Such a DEM model is shown in Fig. 1-single damper.

*Discrete Element Method:* The DEM is a discrete simulation method for granular materials. Every particle is considered as an unconstrained moving body only influenced by applied forces, e. g. the particle–particle and particle–wall contact forces. The dynamics are described by *Newton’s and Euler’s* equation of motion for every particle [23]. This results in general in a coupled nonlinear differential equation with  $6n_p$  degrees of freedom for 3D simulations with  $n_p$  being the number of particles. Here, the algorithms presented in [11] are used.

*Complex power:* To analyze the energy dissipation and the efficiency of the particle damper, the complex power method, introduced by Yang [24], is used. The complex power is determined to  $P = 0.5 F^{*\top} \bar{V}^*$ . Hereby,  $F^*$  denotes the complex amplitude calculated by the *fast Fourier transform* (FFT) of the driving force signal acting on the container and  $\bar{V}^*$  is the conjugate complex amplitude by FFT of the velocity signal of the container motion. The dissipated energy per cycle  $\tilde{E}_{\text{diss}}$  follows from the complex power to  $\tilde{E}_{\text{diss}} = 2\pi E_{\text{diss}} = 2\pi \text{Real}(P)/\Omega$ . To judge about the damper’s efficiency the reduced loss factor  $\eta^*$  [14] is utilized. It is calculated by a scaling of the dissipated energy with the kinetic energy of the particle system  $E_{\text{kin}} = 0.5 m_{\text{bed}} |V_{\Omega}^*|^2$  using the mass of the particle bed  $m_{\text{bed}}$ , i. e. the mass of all particles, to  $\eta^* = E_{\text{diss}}/E_{\text{kin}}$  with  $V_{\Omega}^*$  being the complex amplitude of the velocity signal at driving frequency. As consequence, the reduced loss factor is independent of the container and particle mass and enables the comparison of different particle settings.

### 2.3 Level III

The **third level** of the toolchain, see Fig. 1-structural integration, represents the integration of particle dampers in a vibrating structure to evaluate their overall damping effect. This can be done experimentally or numerically. For simplicity on this level, only 2D motion is considered in this project, i. e. either horizontal or vertical vibrations. For the numerical investigations, three different approaches have been developed. In the first approach, the complete DEM model describing the particle damper used on **level II** is coupled with the dynamical model of the structure. The flexible structure might be described by a reduced linear finite element model or a flexible multibody system. While this approach is very accurate and useful for verification purposes, it is computationally very expensive. Alternatively, the flexible structure model can be coupled with the effective fields or the analytical formulas previous determined in **level II**. This coupling is easily implemented and leads to accurate results and short computation times, see [7, 12] for detailed information about the coupling process. If an analytical formula is present, it even might be used for a damper optimization.

In the following, the toolchain is applied to design different particle damper systems for various application fields and their results are presented.

### 3 Horizontal Vibration Systems of Low Vibration Intensity

Low vibration intensity is defined here as a vibration with particle damper acceleration amplitudes below the gravitational acceleration  $A < g$  and frequencies/eigenfrequencies of  $f_0 < 5 \text{ Hz}$ . Often, only small energy dissipation rates are obtained for such systems so far, due to sticking of particles. Hence, a new and more efficient design of particle dampers is necessary for these applications, whereby the focus is on horizontal vibrations. The proposed design makes use of the rolling property of spheres inside particle containers with flat bases, see [15]. The presentation of this chapter is based on [7, 13, 15].

#### 3.1 Level II—Considerations

The experimental setup to analyze the particle damper's motion modes and energy dissipation under horizontal forced vibration of low intensity is shown in Fig. 4-top. For this purpose, a linear drive is used.

The cuboid container is filled with 36 spherical steel particles of 5 mm radius with clearance  $h_{\text{roll}}$  to the other container side. The container is mounted via a force transducer on a linear drive. Thus, the excitation force acting on the particle container is measured. During the conducted experiments, two different motion modes of the particle bed are observed. Trajectories of these motion modes, obtained from DEM simulations, are shown in Fig. 5. The reduced loss factor, i. e. the efficiency factor of the particle bed, is shown in Fig. 4-bottom. For low excitation amplitudes  $X < X_{\text{rol}}^{\text{opt}}$ , the system is in the so-called *scattering* motion mode. No regular or synchronous motion of the particles is observed, see also Fig. 5a. Hence, only a little amount of energy dissipates, resulting in a low reduced loss factor. When the container amplitude reaches a certain threshold amplitude  $X_{\text{rol}}^{\text{opt}}$  the system turns suddenly into the *rolling collect-and-collide* motion mode, i. e. for  $X > X_{\text{rol}}^{\text{opt}}$ . Here, the particle bed stays together as one particle block and slides and rolls over the container base. The collisions with the container walls are inelastic, i. e. after impact, the particle bed adopts the container's velocity and does not rebound from it. This happens due to multiple inter-particle collisions during impact, see [25, 26] for further details. Hence, a synchronous particle motion with the container is achieved, see Fig. 5b. This leads to a high energy dissipation at  $X = X_{\text{rol}}^{\text{opt}}$  with a slight decrease to higher excitations amplitudes. Equipping the container with buffered walls, making the particle damper hybrid, does not influence its energy dissipation but leads to a considerable noise reduction for this excitation regime.

The numerical DEM results for the reduced loss factor are also pictured in Fig. 4. For the scattered motion mode, i. e.  $X < X_{\text{rol}}^{\text{opt}}$ , the results are on the same scale as the experimental results. However, neither a qualitative nor quantitative agreement of the observed curves for this area is achieved. For the rolling collect-and-collide

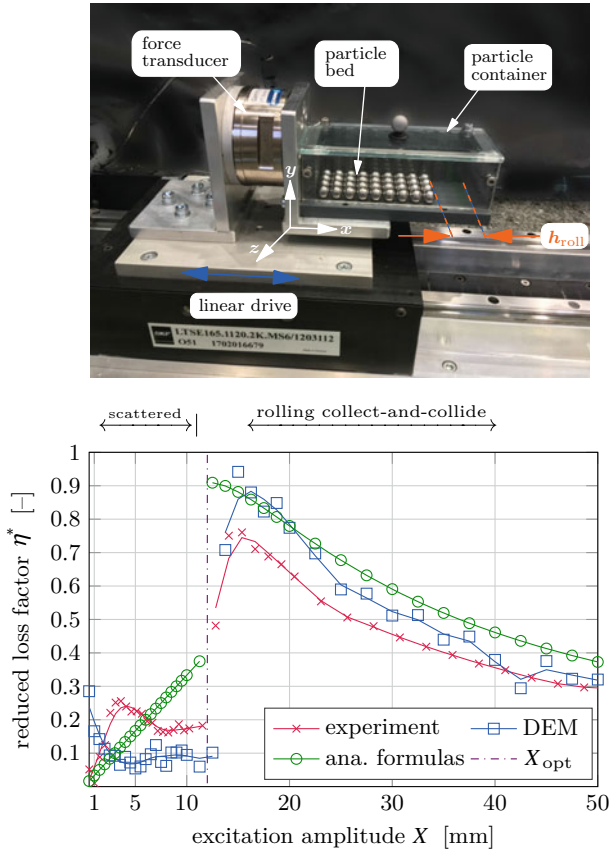


**Fig. 4** Horizontal vibrations analysis of low vibration intensities with experimental setup (top) and corresponding reduced loss factor for an excitation frequency of  $f = 2$  Hz (bottom)

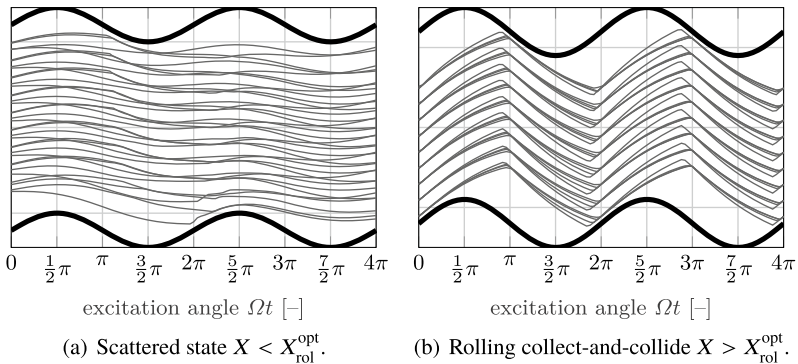


**Fig. 5** Particles trajectories obtained from DEM simulations of particle setting shown in Fig. 4 for different container strokes



motion mode, i. e.  $X > X_{\text{rol}}^{\text{opt}}$ , a good qualitative agreement with the experiments is obtained.

For the scattered state, an empirical formula describing the energy dissipation is found, yielding a rough approximation. For the rolling collect-and-collide regime, instead, an deterministic equation for the energy dissipation is derived. For this analytical equation, the curve progression of the reduced loss factor agrees well with the experiments, see Fig. 4. However, the obtained reduced loss factor values are above the experimentally measured ones for all excitation amplitudes. Additionally, a simple expression for the optimal stroke is achieved to  $X_{\text{rol}}^{\text{opt}} \approx 0.4 h_{\text{roll}}$ , see also Fig. 4. This formula is in great agreement with experimental results [15] and enables a quick and reliable damper design for a structural integration.

Additionally, intensive sensitivity analyses are performed experimentally and numerically in [15]. Most of the particle properties, like Young's modulus, density, coefficient of restitution, or particle number have a negligible influence on the damper's efficiency. However, it turns out that a low friction coefficient and a high particle radius are beneficial. Also, a tilt around the damper's axis are studied. Hereby, a little tilt around the dampers yaw axis is showing only little influence on the damper's efficiency. Indeed, a tilt around its longitudinal or pitch axis might significantly decrease the efficiency of the rolling collect-and-collide motion mode. Finally, the container shape is analyzed. The cuboid shape is replaced by a cylindrical shape heading against gravity. While the efficiency of the damper is only a little reduced, this cylindrical shape is showing the great advantage of applying to vibrations in the whole horizontal plane. Thus, this new efficient damper design for low acceleration vibrations opens a completely new area of applications for particle dampers in mechanical and civil engineering, like the damping of high-rise buildings or wind power plants [15].

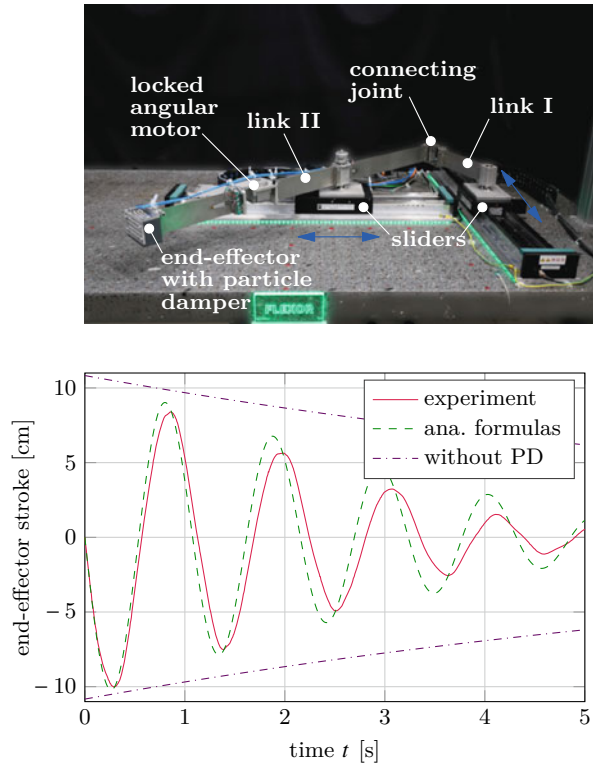
## 3.2 Level III—Considerations

To show the applicability of the derived damper design, it is applied to free and forced vibrations in the following.

### 3.2.1 Free Vibrations

The system to be damped for these vibration intensities is a parallel lightweight manipulator with highly elastic links [7], see Fig. 6-top. The lightweight manipulator consists of two linear motors set up in a "T-configuration". Elastic links, made of spring steel, are mounted via revolute joints on both sliders and are connected via a third revolute joint forming a parallel robot. At the end of link II, the end-effector is mounted, which consists of the hybrid particle damper of multiple layers. The elastic deformation in link II is introduced via the rigid body motion, i. e. when the linear drives are moving, and is dominated by the first (bending) eigenmode.

**Fig. 6** Parallel lightweight manipulator used for harmonic vibration analyses with overview of the system (*top*) and comparison of the end-effector movement for the optimized particle damper (*bottom*)



For this system, all three particle damper models, i. e. full DEM model, effective fields, and analytical formulas, are coupled to the modal reduced model of the system. All coupled models are showing a good agreement to experimental measurements [7]. Finally, the analytical formulas are used to optimize the filling ratio of the different particle damper layers for an initial deflection of link II. The effectiveness of the optimized design is demonstrated experimentally as shown in Fig. 6-*bottom*. Only a small difference between experiment and analytical formulas is found and the system is greatly damped compared to the undamped case.

### 3.2.2 Forced Vibrations

For the forced vibrations, a simple beam-like structure is used as an application example, see Fig. 7-*top*. Its base point is subjected to a harmonic motion of variable frequency using a linear drive. The particle damper is mounted at the tip of the beam and its velocity is measured using a laser scanning vibrometer. Thus, the *frequency response function* (FRF)  $|H^*(f)| = |X_c^*(f)/U^*(f)|$ , with complex particle damper amplitude  $X_c^*$  and complex excitation amplitude  $U^*$  is obtained

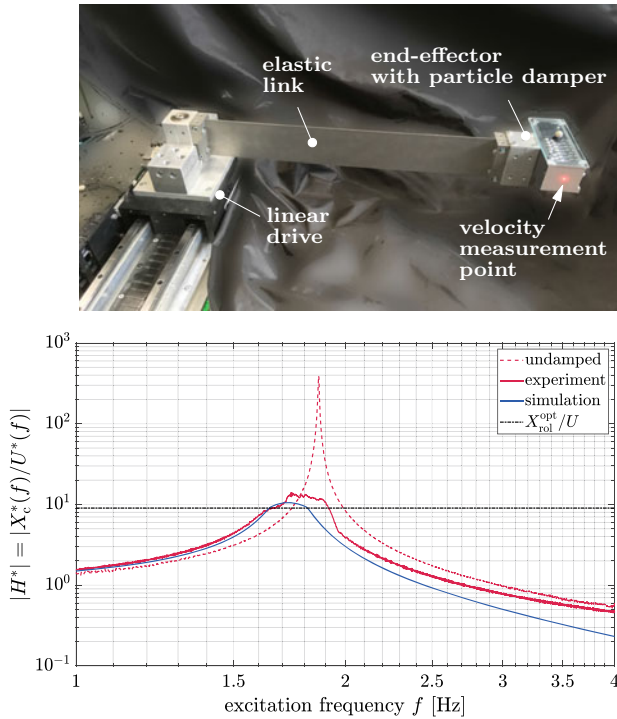


**Fig. 7** Simple beam-like structure setup for forced vibration analyses with overview of system (*top*) and FRF's of optimized particle damper for an excitation of  $U = 1.33$  mm and 36 steel particles of 5 mm radius (*bottom*)

experimentally. Numerically, the equations describing the energy dissipation of the particle damper, which are shown in the normalized form in Fig. 4-*bottom*, are coupled to a modal reduced model of the structure. A good agreement between analytical and experimental obtained frequency response function is achieved for various excitation intensities, validating the presented approach, see [13] for a detailed discussion.

Finally, the coupled model is used to calculate the design parameter of the particle damper to operate it at its maximum efficiency, i. e. at  $X_{rol}^{opt}$  see Fig. 4-*bottom*. A simple analytical expression is obtained. Its accuracy is proven by comparison to an experiment as shown in Fig. 7-*bottom*. Simulation and experiment are only slightly crossing the optimal normalized amplitude of  $X_{rol}^{opt}/U$ , with  $U$  being the excitation amplitude. However, due to uncertainties within the experimental setup, some differences remain in the obtained FRF's. Still, the derived formula provides a powerful tool to design particle damper for applications of low acceleration intensity, see the discussion in [7].

## 4 Horizontal and Vertical Vibration Systems of High Vibration Intensity

High intensity vibrations are defined here as vibrations with an acceleration amplitude  $A \gg g$  and (eigen)frequencies  $f_0 \gg 10 \text{ Hz}$ . For such vibrations, the particle dynamics completely change compared to the previous two sections, but the influence of the gravitational acceleration becomes less.

### 4.1 Level II—Considerations

For the analysis of motion modes and effective fields, a corresponding testbed is developed [9–11, 14] as shown in Fig. 8. The cylindrical particle container is excited by a controlled harmonic force via a shaker perpendicular to gravity. The excitation force is controlled in such a way that the vibration frequency and acceleration magnitude of the container stays constant. The force sensor is mounted between particle container and shaker. The velocity of the particle container is measured via a laser vibrometer.

Filling the particle container with steel spheres of macroscopic size, i. e. from 0.3–5 mm radius, five different motion modes can be observed, as shown as velocity fields in Fig. 9. In Fig. 10 the reduced loss factor and the distribution of motion modes for such a setting are plotted. The solid-like state, see Fig. 9a, is characterized by almost no relative motion between particles and container. This causes the granular matter to look like an added block, staying at the container base and moving with the same velocity as the container. Hence, only little dissipation rates are obtained, see Fig. 10. For the local fluidization, see Fig. 9b, particles located at the top surface become fluidized. Here small to medium dissipation rates are achieved, see Fig. 10. When the whole particle system gets fluidized, the global-fluidization is obtained, as

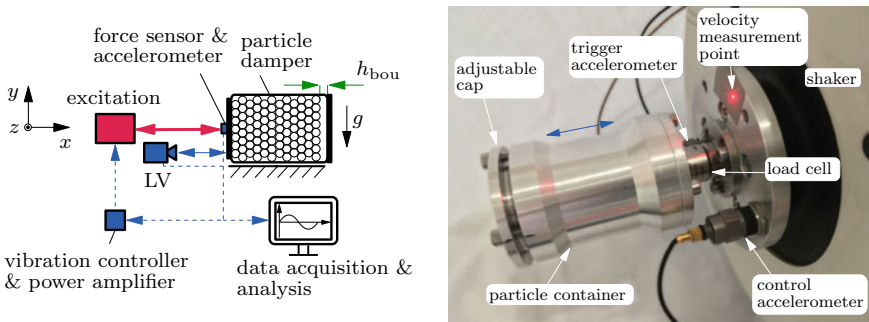


**Fig. 8** Testbed for determination of effective fields of particle damper for high vibration intensities with schematic representation (left) and picture (right)

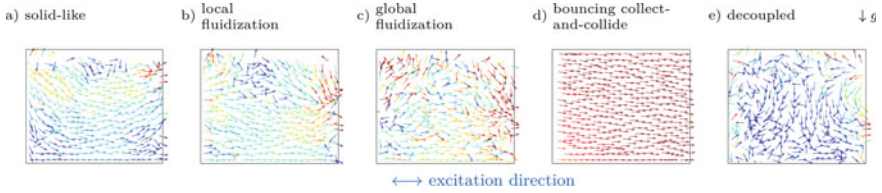
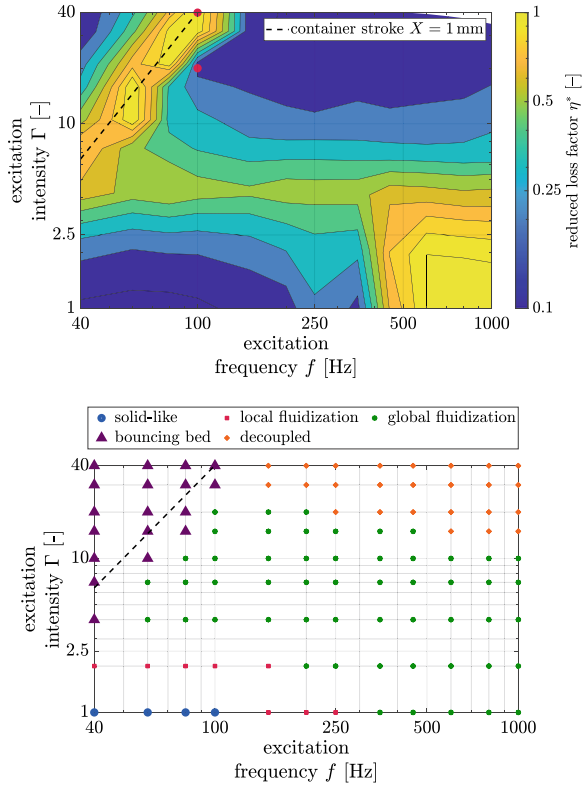


**Fig. 9** Velocity fields of motion modes for high excitation intensities for particle damper shown in Fig. 8. The colors show the magnitude of the in-plane particle velocity normed by the container velocity  $V$  from low (blue) to high (red)

**Fig. 10** Experimentally determined reduced loss factor (*top*) and numerically obtained motion modes (*bottom*) of particle container for horizontal high excitation intensities shown in Fig. 8



shown in Fig. 9c. Medium to high reduced loss factors are seen. Within the bouncing collect-and-collide motion mode, see Fig. 9d, the particles move as one single particle block synchronously with the driven particle container and collide in elastically with the container walls, leading to medium to high reduced loss factors. The decoupled motion mode is shown in Fig. 9e. It is characterized by a very small absolute particle velocity compared to the velocity of the container. Thus, the granular matter appears to be decoupled from the container and results in small dissipation rates.

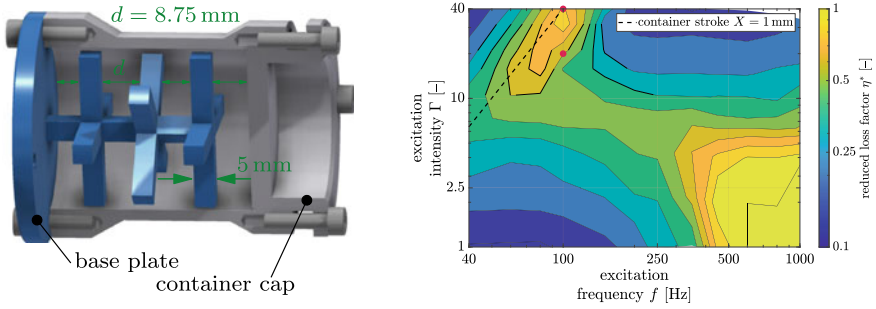


**Fig. 11** Inner structures used for high excitation vibrations with schematic representation (*left*) and result for same particle setting as used in Fig. 10 equipped with inner structure (*right*)

An intensive sensitivity analysis is performed experimentally and numerically in [14] on different particle and container properties affecting the motion modes. The bouncing collect-and-collide motion mode is rather insensitive except for the clearance  $h_{\text{bou}}$ . High reduced loss factor values are again obtained along a constant container stroke of  $X_{\text{bou}}^{\text{opt}} = h_{\text{bou}}/\pi$ , see also Fig. 8 for the definition of  $h_{\text{bou}}$ . For the global fluidization, a high filling ratio of the particle container and a small particle size are found to be advantageous.

*Hybrid Particle Dampers:* In [27] two hybrid particle damper approaches are presented to make the damping behavior around high reduced loss factor values more robust and efficient compared to a pure particle damper. These findings [27] are summarized here. The first approach uses inner structures inside the particle container, see Fig. 11-*left* for a schematic representation. In Fig. 11-*right* the corresponding reduced loss factor is shown. Hereby, the same particle settings as for Fig. 10 are used. Inner structures lead to lower reduced loss factors of the bouncing collect-and-collide motion mode, but to a more robust (wider) behavior in this excitation area, compare red dots in Figs. 10 and 11. Also, they lead to higher reduced loss factors at high frequencies. The more inner structures are used and the smaller the particle radius, the stronger the effect on the reduced loss factor. The second approach presented in [27] utilizes buffered walls of the particle container. The approach aims to influence the local fluidization mode, such that a similar motion as in the bouncing collect-and-collide is achieved. Instead of taking off the container base and flying through the container as for the bouncing collect-and-collide motion mode, the particle bed penetrates the buffered wall material. When the buffered material is completely compressed, an inelastic collision with the container's wall occurs and the relative velocity between particles and wall vanishes. This produces a new particle motion, also called compression collect-and-collide. In Fig. 12-*left*, the corresponding velocity field obtained from DEM simulations is shown. In contrast to the local fluidization mode, a much higher particle velocity is achieved, compare with Fig. 9b. An analytical formula based on Hertz impact theory has been derived, enabling a fast dimensioning of the buffered wall material, see [27]. In Fig. 12-*right*, the reduced loss factor is shown for the particle setting of Fig. 10 using buffered walls

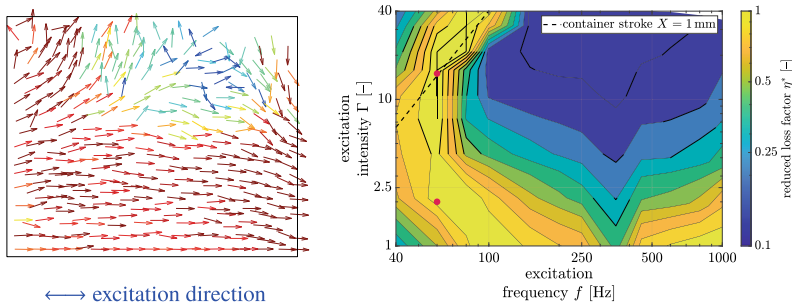


**Fig. 12** Buffered walls used for high excitation vibrations with particle damper's velocity field (*left*) and reduced loss factor for same particle setting as used in Fig. 10 equipped with buffered walls designed for  $f = 60$  Hz (*right*)

designed for an excitation frequency of  $f = 60$  Hz. Here, a very robust behavior of the reduced loss factor concerning the excitation intensity at the desired excitation frequency is achieved.

## 4.2 Level III—Considerations

In the next step, the particle container of **level II** is coupled to an underlying structure as presented in detail in [11, 12]. The previous experimentally and numerically determined effective fields or the full DEM model are used to predict the overall damping of the system. As an application example, a beam-like structure with free-free boundary condition is used. A picture and a schematic representation of the beam and testbed are shown in Fig. 13. The testbed consists of a flexible beam with a hollow profile supported by three soft cables. The beam is excited in the transverse direction with a variable force by a shaker at its free end using a sine sweep excitation. The particle container can be placed at any desired position on the beam. For the investigated analysis here, the container is placed at the free, not excited end, as shown in Fig. 13. Later on, the position of the particle damper can be varied.

Coupling the effective fields of the particle damper to a modal reduced model of the beam, various investigations have been conducted to show its qualitative accuracy and efficiency [11, 12]. In Fig. 14 an exemplary result of this coupling procedure is shown. While a perfect quantitative fit is not obtained, so gives the qualitative results useful guidelines during the particle damper design process. The position of the particle damper plays an important role. Placing the particle damper at an antinode of the shape function a good agreement between damping prediction and the experimental result is achieved. By placing the damper at a position where the shape function exhibits an additional rotation, the damping prediction is still acceptable. Although, in some cases this greatly reduces the energy dissipation of the damper, i. e. for the bouncing collect-and-collide motion mode. Even multiple eigenmodes

**Fig. 13** Testbed to determine the overall damping behavior of the particle damper for high excitation vibrations with schematic representation (top) and picture (bottom)

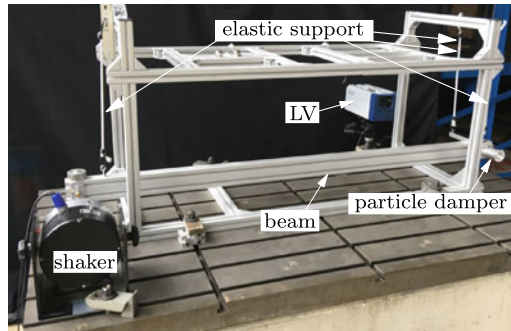
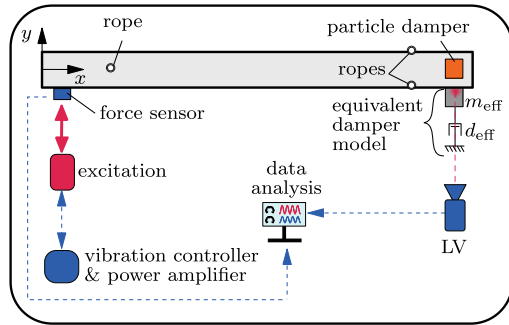
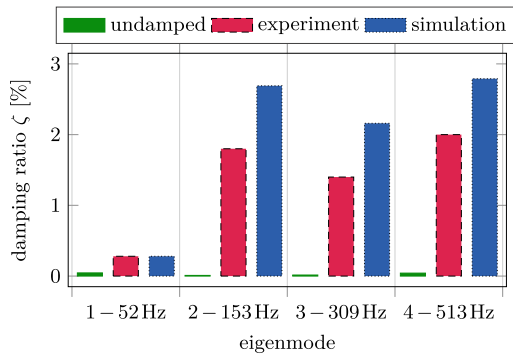


**Fig. 14** Damping ratios of beam-like structure equipped with particle damper of Fig. 8 for high excitation intensities



can be damped efficiently if the particle damper is placed at a position, where these modes have a high shape function value. For further details on the different coupling methods of the numerical models see [11, 12].



## 5 Conclusion

So far particle dampers have been mostly developed by time-consuming experimental-based trial and error strategies for very specific applications, where the adaption to other systems is extremely limited. This might be due to the fact, that the processes in the particle dampers are highly nonlinear and depend on a variety of different influence parameters, like the coefficient of restitution, the coefficient of friction, the excitation frequency, and the vibration amplitude. Due to the lack of understanding of these processes in the dampers and missing systematic design approaches, particle damper's application is so far limited.

The goal of this project is the development of a new design methodology in form of a toolchain for passive vibration damping of lightweight structures and machines using particle dampers. Thereby, using simulations that are verified by experiments, also a deeper understanding of the micro-mechanical processes in the dampers are obtained. This is crucial in the systematic design of particle dampers using numerical methods. By this new design methodology, which is in parts independent of the specific application, it is possible to extend particle dampers to a variety of very different applications, which has been shown at multiple examples.

Using the developed toolchain single particle damper units with predefined characteristics are developed which do not rely on a specific application. Hybrid approaches are used to increase the efficiency of the individual particle dampers. Multiple layers with different filling ratios might be used to obtain an optimized damping behavior for transient vibrations. Inner structures within the dampers cause a more robust behavior and buffering the dampers walls with a polymer leads not only to a considerable noise reduction but can also be used to extend the damper's efficient range of operation for high intensity applications. These individual particle dampers finally form an assembly set, which is ultimately used in the overall damping concept for specific applications.

**Acknowledgements** The authors would like to thank the German Research Foundation (DFG) for the financial support of the project 352324024 during its first project phase, being an associated project to the SPP1897 and for the financial support of the project 424825162 as part of the SPP 1897 during the second project phase.

The authors would also like to thank Dr.-Ing. Marc-André Pick, Dipl.-Ing. Riza Demir, Dipl.-Ing. Norbert Borngräber-Sander and Wolfgang Brennecke for helping to design and realize the experimental rigs.

## References

1. Lu, Z., Wang, Z., Masri, S.F., Lu, X.: Particle impact dampers: past, present, and future. *Struct. Control Health Monitor.* **25**(1), e2058 (2017)
2. Johnson, C.D.: Design of passive damping systems. *J. Mechan. Design* **117**(B), 171–176 (1995)
3. Panossian, H.: Non-obstructive particle damping experience and capabilities. *Proc. SPIE - Int. Soc. Opt. Eng.* **4753**, 936–941 (2002)
4. Simonian, S.S.: Particle beam damper. *Proc. SPIE - Int. Soc. Opt. Eng.* **2445**, 149–160 (1995)

5. Saeki, M.: Impact damping with granular materials in a horizontally vibrating system. *J. Sound Vib.* **251**(1), 153–161 (2002)
6. Chen, T., Mao, K., Huang, X., Wang, M.: Dissipation mechanisms of nonobstructive particle damping using discrete element method. *Proc. SPIE - Int. Soc. Opt. Eng.* **4331**, 294–301 (2001)
7. Meyer, N., Schwartz, C., Morlock, M., Seifried, R.: Systematic design of particle dampers for horizontal vibrations with application to a lightweight manipulator. *J. Sound Vibrat.* **510**, 116319 (2021)
8. Meyer, N.; Seifried, R.: Investigation of the Influence of Parameters on Particle Dampers. *Computational Structures Technology 2018, Sitges, Extended Abstract* (2018)
9. Meyer, N., Seifried, R.: Experimental and numerical investigations on parameters influencing energy dissipation in particle dampers. In: *VI International Conference on Particle-Based Methods - Fundamentals and Applications*, vol. 6, pp. 260–271 (2019)
10. Meyer, N.; Seifried, R.: An experimental model for the analysis of energy dissipation in particle dampers. *PAMM* **19**(1) (2019)
11. Meyer, N., Seifried, R.: Numerical and experimental investigations in the damping behavior of particle dampers attached to a vibrating structure. *Comput. Struct.* **238**, 106281 (2020)
12. Meyer, N., Seifried, R.: Damping prediction of particle dampers for structures under forced vibration using effective fields. *Granul. Matter* **23**(3), 64 (2021)
13. Meyer, N.; Seifried, R.: Optimal design of particle dampers for structures with low first eigenfrequency under forced vibration. In: *7th Edition of the International Conference on Particle-Based Methods*, vol. 7 (2021)
14. Meyer, N., Seifried, R.: Toward a design methodology for particle dampers by analyzing their energy dissipation. *Comput. Particle Mech.* **8**(4), 681–699 (2021)
15. Meyer, N.; Seifried, R.: Energy dissipation in horizontally driven particle dampers of low acceleration intensities. *Nonlinear Dyn.* (2022)
16. Meyer, N., Wagemann, E.L., Jackstadt, A., Seifried, R.: Material and particle size sensitivity analysis on coefficient of restitution in low-velocity normal impacts. *Comput. Particle Mech.* (2022)
17. Stronge, W.J.: *Impact Mechanics*, 2 edn. Cambridge University Press, Cambridge (2018)
18. Pöschel, T., Brilliantov, N.V.: Extremal collision sequences of particles on a line: optimal transmission of kinetic energy. *Phys. Rev. E* **63**(2), 1–9 (2001)
19. Goldsmith, W.: *Impact: The Theory and Physical Behavior of Colliding Solids*. Edward Arnold Publishers, London (1960)
20. Seifried, R., Minamoto, H., Eberhard, P.: Viscoplastic effects occurring in impacts of aluminum and steel bodies and their influence on the coefficient of restitution. *J. Appl. Mech.* **77**(4) (2010)
21. Tataru, Y., Moriwaki, N.: Study on impact of equivalent two bodies: coefficients of restitution of spheres of brass, lead, glass, porcelain and agate, and the material properties. *Bull. JSME* **25**(202), 631–637 (1982)
22. Minamoto, H., Seifried, R., Eberhard, P., Kawamura, S.: Analysis of repeated impacts on a steel rod with visco-plastic material behavior. *Eur. J. Mech. A. Solids* **30**(3), 336–344 (2011)
23. Pöschel, T.: *Computational Granular Dynamics: Models and Algorithms*. Springer, Berlin (2005)
24. Yang, M.Y., Lesieutre, G.A., Hambric, S., Koopmann, G.: Development of a design curve for particle impact dampers. *Noise Control Eng. J.* **53**, 5–13 (2005)
25. Sanchez, M., Rosenthal, G., Pugnali, L.: Universal response of optimal granular damping devices. *J. Sound Vib.* **331**(20), 4389–4394 (2012)
26. Bannerman, M.N., Kollmer, J.E., Sack, A., Heckel, M., Mueller, P., Pöschel, T.: Movers and shakers: granular damping in microgravity. *Phys. Rev. E* **84** (2011)
27. Meyer, N., Seifried, R.: Design of Robust Particle Dampers Using Inner Structures and Buffered Walls. Preprint series of the SPP 1897 Calm, Smooth, Smart, vol. 35, p. 24 (2022)